Estuaries and Coasts (2025) 48:161
https://doi.org/10.1007/s12237-025-01583-4

Soil and Plant Physicochemical Properties Associated with Coastal Marsh Degradation

Jennifer Volk[1] · Cathilyn L. McIntosh[2] · J. Adam Langley[2] · Samantha K. Chapman[2] · Lisa G. Chambers[1]

Received: 25 February 2025 / Revised: 17 June 2025 / Accepted: 30 June 2025

Abstract
Coastal wetlands perform essential ecosystem functions that may be negatively impacted by anthropogenic activities and environmental change. Coastal wetland degradation has been observed in the Tolomato River estuary, part of the Guana Tolomato Matanzas National Estuarine Research Reserve (GTMNERR), on the east coast of Florida (USA). While some portions of marsh have well-consolidated soil (i.e., "stable"), others have reduced plant vigor and unconsolidated soils (i.e., "unstable"). We quantified how elevation, plant biomass, and soil biogeochemical properties (particle size, organic matter content, sulfide, total and dissolved nitrogen and phosphorus, and potassium permanganate oxidizable carbon (POXC)) differed between stable and unstable marsh soils. Three sites, each containing triplicate stable and unstable plots, were identified for study; a fourth site with only stable plots served as a reference condition. Soil cores (0–30 cm) were collected from each plot (21 total) and analyzed. Results indicated ammonium and sulfide concentrations averaged 64% and 28% higher in unstable soils than stable, respectively. Organic matter content, total carbon, total nitrogen, and POXC were all 10–15% greater in stable soils. Root productivity, soil resistance, and elevation were also 267%, 200%, and 0.17 m higher in stable soils. Our findings suggest land managers can use visual and tactile cues of marsh stability to rapidly assess plant and soil physicochemical properties, allowing for informed decision making regarding the need for protection and restoration.

Keywords Wetlands · Biogeochemistry · *Sporobolus alterniflorus* · Soil

Introduction

Wetlands are ecologically and economically valuable ecosystems because they prevent shoreline erosion, act as a carbon (C) sink, and filter out pollutants (Bertolini & da Mosto, 2021). While wetlands constitute only 6–9% of the Earth's land surface, they store up to 35% of the global land C pool in their soil by absorbing more CO_2 than they release (Deng et al., 2022). Natural and managed wetlands can also treat wastewater and sequester nutrients (Almuktar et al., 2018; Zedler & Kercher, 2005), helping to prevent algal blooms and fish kills due to excess nitrogen (N) and phosphorus (P) input. Coastal salt marshes, a type of wetland that is tidally influenced, are some of the most productive ecosystems in the world and offer habitat for many fish and bird species (Kennish, 2001; NOAA, 2024). While wetlands mitigate anthropogenic impacts and provide essential ecosystem services, ongoing degradation of these ecosystems inhibits their functions (Barbier, 2013).

In the twentieth century, coastal wetland area declined 60% worldwide (Davidson, 2014) owing to land use change, altered hydrology, human population growth, and sea level rise (Xu et al., 2020). In addition, coastal wetland loss has occurred due to canal and dam construction, agriculture, pollution, boat wakes, introduced species, and hurricanes. These factors have led to a loss of sediment, changes in tidal dynamics, erosion, and plant death (Kennish, 2001). In the USA, Florida harbors more land surface area of wetlands than the rest of the conterminous states, but it has lost half of its wetlands, including coastal wetlands, in the past

Communicated by Just Cebrian

Jennifer Volk and Cathilyn L. McIntosh contributed equally to the research and are co-first authors.

✉ Lisa G. Chambers
lisa.chambers@ucf.edu

[1] Department of Biology, University of Central Florida, Orlando, USA

[2] Department of Biology and Center for Biodiversity & Ecosystem Stewardship, Villanova University, Villanova, PA, USA

Published online: 11 August 2025

200 years (Clark et al., 2010; Haag & Lee, 2010). Wetland research and restoration efforts have accelerated in recent years, driven by a growing awareness of this rapid decline (Bertolini & da Mosto, 2021).

The Guana Tolomato Matanzas National Estuarine Research Reserve (GTMNERR), located in St. Augustine, Florida, encompasses 76,760 acres of land, including vast coastal wetlands at risk of decline (NOAA, 2024). In recent years, land managers and scientists have observed regions of apparent marsh degradation (e.g., decreased plant cover, increased prevalence of open-water ponds, and soil collapse) along the Tolomato River in the GTMNERR, but the cause is unknown (Endris et al., 2023; Price, 2006). Understanding how these visible cues relate to soil and plant characteristics in degraded and healthy marshes is paramount for future research and coastal restoration efforts in this region.

Plant biomass and biogeochemical soil analyses can provide insight on nutrient cycling, productivity, and oxidation–reduction status, allowing land managers at the GTMNERR to equate visual wetland decline (loss of vegetation cover, increased soupy soil, and subsequent conversion to open water) to quantifiable physical and biogeochemical parameters. For example, observable declines in plant height or coverage could be indicative of elevated sulfide (S^{2-}). Produced as a byproduct of sulfate reduction, S^{2-} can be toxic to plant species, such as *Sporobolus alterniflorus* (Lamers et al., 2013). Since seawater contains sulfate ions, salt marshes under conditions of waterlogging and stagnation (low flushing) could promote increased rates of sulfate reduction, the accumulation of S^{2-}, and a subsequent vegetation decline from root stress (Koch et al., 1990; Morris, 1980). Moreover, persistent ponds of standing water could indicate prolonged anaerobic conditions, which can cause ammonium (NH_4^+), produced through the mineralization of organic N compounds, to accumulate (Morris, 1984; Hessini et al., 2017); Lamba et al., 2017). Since NH_4^+ is a source of nutrients for many wetland plants, high concentrations of available NH_4^+ in the soil may also indicate low nutrient uptake from plants due to stress or a lack of dry-down conditions to facilitate nitrification (Morris, 1980; Morris, 1984; Hessini et al., 2017; Lamba et al., 2017). Conversely, high nitrate (NO_3^-) concentrations may suggest more aerobic conditions and high rates of nitrification (Reddy & DeLaune, 2008). High NO_3^- concentrations have also been associated with salt marsh loss due to stimulated microbial activity decomposing organic compounds (Deegan et al., 2012).

Characteristics of the organic and inorganic components of the soil may also cause or respond to wetland decline. Wetland soils form organic matter (OM) when the rate of primary productivity exceeds the rate of decomposition (Reddy & DeLaune, 2008). Therefore, high soil OM content suggests plant detritus and other organic inputs have not fully decomposed but instead accumulate in the soil; this accumulation is often attributed to anaerobic soil conditions slowing C respiration (Bot & Benites, 2005). Carbon is the primary constituent of soil OM (Bennett & Chambers, 2023; Breithaupt et al., 2023), and potassium permanganate oxidizable carbon (POXC) represents a specific portion of the C pool—the amount of C that is semi-labile in the soil (Culman, et al. 2021). Both OM content and POXC may serve as indicators of soil health or inundation conditions. For example, increased flooding creates more reduced soil conditions and slower mineralization rates, which could promote the accumulation of soil OM, including the minimally processed POXC pool (Chambers et al., 2024). Meanwhile, the inorganic portion of wetland soils is characterized by grain size, such as clay, silt, and sand. Higher clay and silt content is associated with slower water infiltration rates and may create more stagnant, anaerobic conditions when abundant; this higher hydrological resistance could contribute to S^{2-} toxicity, nutrient accumulation, and plant stress. Conversely, sand is associated with higher water infiltration rates and may allow more flushing of water and nutrients through the pore spaces (Giap et al., 2021).

Differences in plant height and cover can be visually apparent in coastal marshes and thus useful to coastal land managers, but the utility of these indicators in predicting marsh health and resilience requires empirical evaluation. For example, aboveground and belowground biomass can be decoupled, such that high nutrient availability can promote photosynthetic tissue production, while concurrently reducing the relative allocation to roots (Wang et al., 2024). This belowground biomass, consisting of both root and rhizome matter, is critical to enhancing soil strength by forming dense root mats that trap sediment and organic matter (Vincent et al., 2013; Moseman-Valtierra et al. 2016; Cahoon et al., 2021), ultimately supporting the marsh platform (Chambers et al., 2019). Reductions in belowground biomass, or disturbance of sediment beneath root zones, have been linked to sediment resuspension and significant marsh loss (Chambers et al., 2019; Nyman et al., 1994; Turner, 2011). Soil resistance, measured by a penetrometer, can assess the degree of soil compaction, providing quantitative evidence of how cohesive and stable the soil structure is, which is often directly related to belowground production (Day et al., 2011; Sasser et al., 2018).

Elevation and sea level rise are also important factors governing wetland sustainability. As sea level rise accelerates, and wetlands fail to compensate with elevation gain through sediment and organic matter accumulation, the frequency, duration, and depth of inundation increase (Cahoon, 2015; Cahoon et al., 2019; Raposa et al., 2016; Reed, 1995). When this occurs, coastal wetlands turn into unvegetated mudflats with open water (Morris et al., 2002; Orson et al., 1985). On the east coast of Florida, the rate of sea level rise has been recorded at 2–3 mm per year between 1854 and

1999 (Zervas, 2001), with more recent studies suggesting an acceleration in the rate of rise (Parkinson & Wdowinski, 2022). Past modeling of sea level rise scenarios in the GTMNEER indicates the tidal wetlands with productive marsh vegetation far from tidal creeks are likely to migrate upland in response to sea level with minimal aerial loss, while other areas of marsh must accelerate vertical accretion to prevent conversion to open water (Bacopoulos et al., 2019). Wetlands may fail to accumulate elevation due to lower root productivity, increased temperatures, increased nutrient input, decreased soil strength, and erosion (Deegan et al., 2012; Langley et al., 2009; Turner, 2011; Wigand et al., 2014). Previous research demonstrates heightened soil inundation can deteriorate the organic soil matrix, causing excessive swelling and sediment resuspension (Chambers et al., 2019; Nyman et al., 1994) and preventing soil consolidation (Boudreau et al. 2024). Excessive waterlogging can also cause plant dieback and lead to a sharp decline in plant biomass in response to flooding (Snedden et al., 2015).

The goal of this observational study was to characterize the soil biogeochemical properties and plant productivity metrics of marsh areas qualitatively deemed to be "stable" (i.e., consolidated-feeling soil and visually high plant cover) and "unstable" (i.e., unconsolidated-feeling soil and visually low plant cover) at four sites along the Tolomato River estuary. Since most land managers, including at the GTMNERR, visually assess their land, the goal of this study was to determine if their visual observations, like unvegetated areas and soupy soils, were indicative of quantitative differences in physicochemical properties in those areas. We hypothesized that unstable wetland soils would have higher concentrations of NH_4^+, S^{2-}, OM, POXC, clay, and silt and lower concentrations of NO_3^- and sand, when compared to stable wetland soils in the GTMNERR. We also hypothesized that unstable soils would have lower root productivity, elevation, and soil resistance compared to stable soils. These results can be used to determine if visual assessment of marsh degradation by land managers is a reliable indicator of certain soil and plant properties.

Methods

Study Site

This study occurred in tidal salt marshes along the Tolomato River Estuary, located in the GTMNERR in St. Augustine, Florida (29.9601, − 81.3168). The Tolomato River basin, covering 218 km^2, is part of the Intracoastal Waterway and is maintained for public navigation (Frazel, 2009). Dredging has changed parts of the river, creating islands covered with varying amounts of vegetation. Several creeks, including Casa Cola, Deep, Smith, Jones, Capo, Stokes, Sweetwater, Marshall, and Sombrero, flow into the Tolomato River, and the outflow is connected to the Atlantic Ocean by the St. Augustine Inlet (Frazel, 2009). The Tolomato River also receives flow from the Guana River, which discharges into the Tolomato River just upstream of the study region.

Four coastal wetland sites were chosen along the Tolomato River between the Guana River and St. Augustine Inlet (Fig. 1). Marsh plot stability was determined qualitatively by visual inspection and feel (with the assistance of a land manager). Specifically, stable plots were identified as having consolidated soil that supports body weight and contains healthy, dense plant cover with intact roots; unstable plots were identified as having soupy soil that does not support body weight and contains sparse vegetation and/or areas of bare sediment. The qualitative characteristics of soil consolidation and visual plant cover were chosen because local citizens and land managers expressed concern that these characteristics may suggest a decline in ecosystem health or differences in ecological properties or functions in these areas (Endris et al., 2023; Price, 2006). All the sites were dominated by *Sporobolus alterniflorus* and were characterized by the existence of large linear berms of dead oyster shells (locally referred to as "oyster rakes") located along the boundary between the river and the marsh. A study investigating historical photographs of dead mounds of oyster shell in the Intracoastal Waterway found the earliest aerial image in 1943 (Grizzle et al. 2002). They argued boat wake activity was correlated with its development, and most of the dead oyster berm had a height of 1 m above the highest water level (Grizzle et al. 2002). Land managers have expressed concern the oyster rakes may be contributing to increased ponding, decreased vegetation, and soupy soil (or may be a symptom of erosion in the area from boat wakes) but have noticed varied conditions in marsh health behind rakes (Price, 2006). Therefore, all four sites chosen for study were located behind notable oyster rakes, and rake presence was not a manipulated factor in this study. Sites 1, 2, and 4 each contained three stable and three unstable plots (six per site) (Fig. 1). Site 3 was the only site without identifiable unstable plots but instead was visually deemed to be an appropriate reference for a highly stable, healthy end member site with 3 stable plots.

Field Methods

At each of the four sites, the six 1-m^2 plots were haphazardly identified (based on the visual and tactile indicators described above for stable vs. unstable conditions), GPS coordinates recorded, and plots marked with a PVC pole. At each site, all plots were situated 1–3 m landward of the oyster rake. The average distance between plots within a site was approximately 20 m.

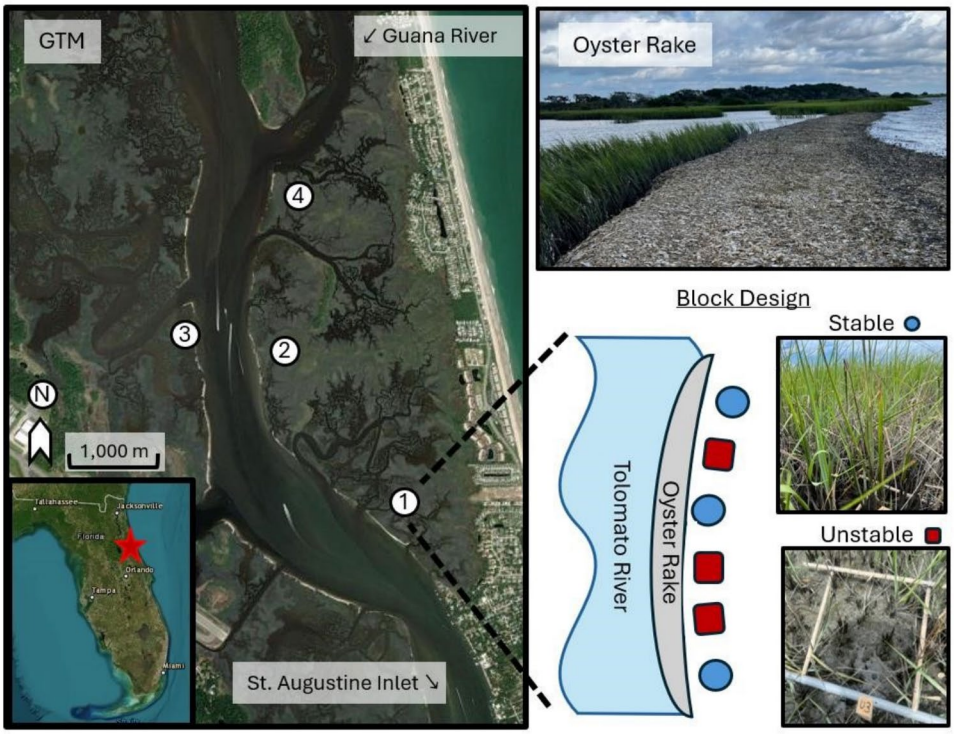

Fig. 1 Overview of site location and experimental design. Inset map highlights the location of the Guana Tolomato Matanzas National Estuarine Research Reserve (GTMNERR) in northeastern Florida, with site locations numbered as 1, 2, 3, and 4 (left panel). The upper right panel shows an image of an oyster rake, a seminatural berm of dead oyster shells, along the edge of a salt marsh shelf within the Intracoastal Waterway, behind which all study sites are located. The lower right panel illustrates the block design for sites 1, 2, and 4, with stable ($N=3$) and unstable ($N=3$) plot types assigned approximately 1–3 m behind an oyster rake. Site 3 is assigned only three stable plots. Left panel and inset map retrieved from NAIP USGS

Soil cores were collected from each plot at all 4 sites (21 total cores) on September 1 and 22, 2023, and analyzed at the Aquatic Biogeochemistry Laboratory at the University of Central Florida. To obtain soil samples, either a 10- or 7-cm-diameter beveled polycarbonate tube was hammered into the soil with a rubber mallet and wooden block. Although compaction can be an issue when collecting soil cores, none was noted during sampling. The soil was extruded and segmented into three depths: 0–10 cm, 10–20 cm, and 20–30 cm (Harttung et al., 2021). Each sample was placed in an airtight polyethylene bag and put on ice for transport to the laboratory.

At the lab, the samples were dried and then weighed for bulk density (BD) calculation and stored at 4 °C before analysis (Harttung et al., 2021). All soil biogeochemical analyses described below were conducted on each plot and depth segment ($n=64$).

Soil resistance was measured using a custom-built in situ sliding hammer flat cone penetrometer. Instrument dimensions are comparable to those outlined by Twohig and Stolt (2011). In February and May 2024, three penetrometer measurements were taken outside selected plots to avoid influencing plant or elevation measurements. The average of these measurements was then calculated to determine the mean soil resistance. Each measurement involved dropping a 2.27 kg weight five times. The final depth reached by the penetrometer, denoted as Δz (cm), was used to estimate soil resistance, R_a (pascals), according to Eq. 1 (Sanglerat, 1972).

$$\mathrm{Ra} = \frac{Mgh}{A\Delta z} * \frac{M}{M+m} \tag{1}$$

Variable A accounts for the area of the flat bottom cone (m^2). The mass of the weight used to drive the penetrometer through the soil is represented by M (kg), and the mass of the instrument's shaft is represented by m (kg). The height from which the weight is dropped is represented by h (m), and g stands for the gravitational constant (m/s^2). The equation assumes that any energy lost during the process is absorbed by the shaft and is not considered separately. It also assumes minimal friction between the instrument and the soil and does not consider the mass of soil displaced during the measurement. A more complete description of the formula is found in Minasny (2012).

Elevation was measured in May 2024 using a GPS-real-time kinematic positioning system (Emlid Reach RS2+) mounted on a 2-m survey-grade pole and outfitted with a flat rounded bottom about 6 cm in diameter. The module was connected to the District 2 St. Johns County Florida base station and used the NAVD88 Florida East coordinate system. Measurements were corrected by the receiver using the base station's known elevation (2770.3 cm NAVD88). Three measurements were made per plot and averaged together to obtain the mean elevation. For each measurement, the pole

was positioned flush with the marsh surface and oriented perpendicularly using a bubble level attached to the survey pole. In cases when the soil could not support the weight of the unit, the pole was held at the point of initial resistance.

Stem height, live standing stem density, and number of dead stems of *S. alterniflorus* were measured at sites 1 and 2 in July 2023 and site 4 in October 2023. Cumulative plant height (cm) per plot was calculated by multiplying average stem density (stem number per area) and average stem height. This index was most predictive in differentiating stable and unstable plots. Root productivity was measured using root ingrowth bags (5 cm in diameter, 30 cm in length), which were placed vertically to a 30 cm depth in each plot in April 2023 and retrieved 6 months later in October 2023. Bags were filled with sphagnum peat moss (Premier Horticulture Inc.) and made from 1-cm nylon mesh to allow root ingress. Once collected, bags were stored at 4 °C in the lab at Villanova University. Roots present on the exterior of the root bag were removed. Large debris and peat were removed by washing the roots with a 19.05-mm sieve on top of a 2-mm sieve. During a time span of 5 min, larger roots were picked out (> 2 mm), and during a time span of 15 min, smaller roots (< 2 mm) were collected. Wet root mass was weighed, dried for 3 days, and reweighed to obtain dry weight. Productivity was calculated using Eq. 2 and was reported as g m^{-2} mo^{-1}.

$$RP = \frac{Root\ dry\ weight}{(Bag\ volume * time\ deployed} \quad (2)$$

Laboratory Analysis

Soil S^{2-} was quantified by adapting a method from porewater sulfide concentrations (Castañeda-Moya et al., 2013; McKee et al., 1988). In the field, 7 mL of antioxidant buffer was pipetted in 20-mL glass scintillation vials, approximately 1 g of soil was added, and the samples were transported on ice to the lab. The redox was analyzed with a LIS-146AGSCM micro sulfide ion electrode the same day of collection (Lazar Research Laboratories, Los Angeles, CA, USA). Other soil samples from the field were exposed to air so the sulfide volatilized. A standard curve with this aerated sample, 7 mL of antioxidant buffer, and known concentrations of sulfide were made in the lab to calculate the unknown concentrations. Soil for sulfide analysis was collected on May 16 and June 3, 2024.

Nitrate + nitrite (NO_3^-), soluble reactive phosphate (SRP), ammonium (NH_4^+), and dissolved organic C (DOC) extractions were conducted within 48 h after soil sampling. Each sample was homogenized; a subsample, between 2 and 4 g of wet soil, was placed into 40-mL centrifuge tubes, and 25 mL of 2 M KCl was added (Steinmuller et al., 2020). The samples were shaken in an orbital shaker for 1 h at 150 rpm and 25 °C, centrifuged for 10 min at 5000 rpm, vacuum filtered through 0.45-µm filters, and preserved by adding 1 drop of double deionized sulfuric acid to achieve a pH < 2 (Steinmuller et al., 2020). The extractable nutrients were quantified on a SEAL AQ2 Automated Discrete Analyzer within 28 days post-extraction at wavelengths 520 nm for NO_3^-, 660 nm for NH_4^+, and 880 nm for SRP (Seal Analytical, Mequon, WI, USA; EPA methods 353.2 Rev. 2.0, 350.1 Rev. 2.0, and 365.1 Rev. 2); DOC was run on a Shimadzu TOC-L Analyzer (Shimadzu Scientific Instruments, Kyoto, Japan).

Bulk soil properties included OM content, mineral particle size, and total C, N, and P content. Organic matter content was determined by drying, grinding, and combusting soils.

Subsamples (35–50 g) were placed on aluminum tins and dried at 70 °C in an oven. After a minimum of 3 days, the samples were placed in a desiccator to cool and then weighed for moisture content calculations (Ho & Chambers, 2020). The soil was ground by mortar and pestle, placed into 20-mL scintillation vials, and ground further with a ceramic ball and a SPEX Sample Prep 8000M Mixer/Mill (SPEX, Metuchen, NJ, USA). Subsamples (less than 0.5 g) were placed in crucibles, weighed, and combusted at 550 °C for 3–4 h in a muffle furnace. The weights of the soil ash were recorded for OM content calculations (Steinmuller et al., 2020). Particle size analysis was performed to assess the proportion of clay, silt, and sand in the soil. Around 1 g of soil ash was placed into centrifuge tubes, and 40 mL of 4% sodium hexametaphosphate was added to break up aggregates. The samples were then vortexed for 10 s and placed on an orbital shaker at 150 rpm for 24 h. The particle size of the soil was quantified by pipetting 3–10 mL of sample into a Cilas 1190 Particle Size Analyzer (CILAS, Orleans, France). Total C and total N were analyzed on approximately 5 mg of dried, ground soil by folding it in tin boats and running it on an Elementar Vario Micro Cube (Elementar Americas Inc., Mount Laurel, NJ, USA). Also, to measure the pH of the soil, a slurry of 5 g of field moist soil and 25 mL of nanopore H_2O were made in disposable beakers, allowed to settle for 30 min, and then analyzed on an Accumet benchtop pH probe (Harttung et al., 2021). Total P of the soil was determined on 0.5 g of dried, combusted soils from the OM analysis, which was placed in 50-mL digestion tubes. Around 50 mL of 1 N HCl was added to the tubes, and the tubes were placed in a digestion block. The liquid was boiled for 30 min at 100 °C, filtered through 42 Whatman filter papers into 50-mL volumetric flasks, filled to volume with nanopore H_2O, and stored in 20-mL scintillation vials until analysis (Andersen, 1976). Total P was analyzed colorimetrically on the SEAL AQ2 Automated Discrete Analyzer within 28 days at 880 nm wavelength (Seal Analytical, Mequon, WI, USA; EPA method 365.1 Rev. 2.).

Potassium permanganate oxidizable carbon (POXC) was analyzed on 1 g of dried, ground soil. The soil was placed into centrifuge tubes, and 10 mL of 0.2 $KMnO_4$ and 10 mL of nanopure H_2O were added. The samples were vortexed for 5 s, placed on an orbital shaker at 150 rpm for 2 min, and centrifuged at 5000 rpm for 10 min at 20 °C. Around 500 µL of the samples were pipetted into scintillation vials, diluted with 20 mL of nanopore H_2O, and inverted to mix (Bhadha et al., 2018; Culman et al., 2021). The diluted samples, around 200 µL, were pipetted into a 96-well plate and run through a BioTek Synergy HTX spectrophotometer (Agilent Technologies, Santa Clara, CA, USA).

Statistical Analyses

Statistical analysis was performed in RStudio (RStudio Inc., Boston, MA, USA; version 4.3.1). Generalized linear mixed models (glmms) were run on each parameter to assess stability as a predictor of that variable. To account for inherent site differences, "site" was treated as a random effect in the model (other effects were fixed). Stability was also a categorical variable (stable or unstable). R equation: Analysis ~ Stability + Depth + (1|Site). Tukey pairwise comparisons were then utilized to assess statistical differences between stable and unstable soil and depth results. Performance tests were conducted through the "performance" package to assess homogeneity of variance, collinearity, normality of residuals, and linearity. The models utilized either a Gaussian or Gamma identity link or log distribution, and transformations like square root and log were conducted to meet the assumptions. If the assumptions could not be met after transformations, Kruskal–Wallis's rank sum tests were performed. Based on those significant results, Dunn's post-hoc comparisons were conducted with the "dunn.test" package. A p-value less than 0.05 was deemed significant. Analyses that used Gamma distribution were as follows: NH_4^+, total carbon, OM content, TP, and soil resistance. Analyses that used Gaussian distribution were as follows: total nitrogen, POXC, clay, silt, sand, sulfide (square root transformed), root productivity (log transformed), elevation, and pH. Analyses that used Kruskal Wallis were as follows: SRP, NO_3^-, and BD. Also, a Pearson correlation matrix was conducted to assess the relationship between stability, as a binary categorical variable, to all the physicochemical analyses, and corresponding p-values were calculated based on those results (RStudio Inc., Boston, MA, USA; version 4.3.1).

Results

Unstable plots had higher concentrations of soil extractable NH_4^+($p = 0.007$), S^{2-} ($p = 0.03$) and total P ($p = 0.01$). Specifically, unstable plots averaged (mean ± standard error) 31.55 ± 5.69 mg NH_4^+ kg^{-1}, 65.94 ± 12.42 mg S^{2-} kg^{-1}, and 0.64 ± 0.05 mg total P g^{-1}. In contrast, stable plots had lower concentrations of these analytes: 19.22 ± 2.35 mg NH_4^+ kg^{-1}, 51.71 ± 6.58 mg S^{2-} kg^{-1}, and 0.54 ± 0.05 mg total P g^{-1} (Figs. 2 and 3). Conversely, stable plots had higher concentrations of total C and N contents than unstable plots ($p = 0.01$ and $p = 0.005$, respectively; Fig. 3). Stable plots averaged 78.95 ± 2.36 mg total C g^{-1} and 4.20 ± 0.13 mg total N g^{-1}, while unstable plots had 68.96 ± 3.65 mg total C g^{-1} and 3.74 ± 0.16 mg total N g^{-1}, respectively. Likewise, soil POXC concentration ($p = 0.02$) and OM content ($p = 0.007$) were higher in stable plots. Soil POXC and OM averaged 18.01 ± 0.55 mg g^{-1} and $22 \pm 0.50\%$ for stable plots and 15.90 ± 0.73 mg g^{-1} and $20 \pm 0.65\%$ for unstable plots, respectively.

Soil particle size (percentages of clay, silt, and sand) did not statistically differ between plot types (all $p > 0.05$; Fig. 4). However, bulk density was higher in unstable plots (0.39 ± 0.01 g cm^{-3}) compared to stable plots (0.35 ± 0.01 g cm^{-3}); $p = 0.02$). In contrast, soil resistance was higher in stable plots (0.03 ± 0.0009 Pa) compared to unstable plots (0.01 ± 0.0004 Pa; $p < 0.001$; Fig. 5). Stable plots also had higher root productivity (37.4 ± 10.35 g m^{-2} mo^{-1}), elevation (0.64 ± 0.02 m), and cumulative plant height (789 ± 54.82 cm) than unstable plots (10.2 ± 4.04 g m^{-2} mo^{-1}, 0.47 ± 0.02 m, and 457 ± 35.84 cm, respectively; all $p < 0.001$; Fig. 5). Also, with depth, NO_3^-, OM, DOC, TN, and TP generally decreased while sulfide and BD generally increased with depth ($p < 0.05$). For the Pearson correlation, soil resistance ($r = 0.627$), root productivity ($r = 0.588$), cumulative height ($r = 0.561$), and elevation ($r = 0.444$) were variables moderately or strongly correlated with differences between stable and unstable soil ($p < 0.0001$).

Discussion

Elevation Is a Key Abiotic Variable Associated with Soil Stability

Stable plots were 0.17 m higher in elevation and had 200% greater soil resistance. These findings, coupled with higher S^{2-} concentrations in unstable soil, indicate increased waterlogging with the lower elevation in unstable soil. Plant biomass can decrease in response to lower elevation and increased inundation. For example, belowground biomass decreased by 90% in a Mississippi River deltaic plain during heightened flooding, reducing soil shear strength and erosional resistance (Snedden et al., 2015). Increased inundation has also been linked to decreased soil strength and increased erosion by resuspending sediments (Chambers et al., 2019; Day et al., 2011; Nyman et al., 1994). Prior research suggests continuous flooding leads to the accumulation of floating detrital material (sometimes termed "floc")

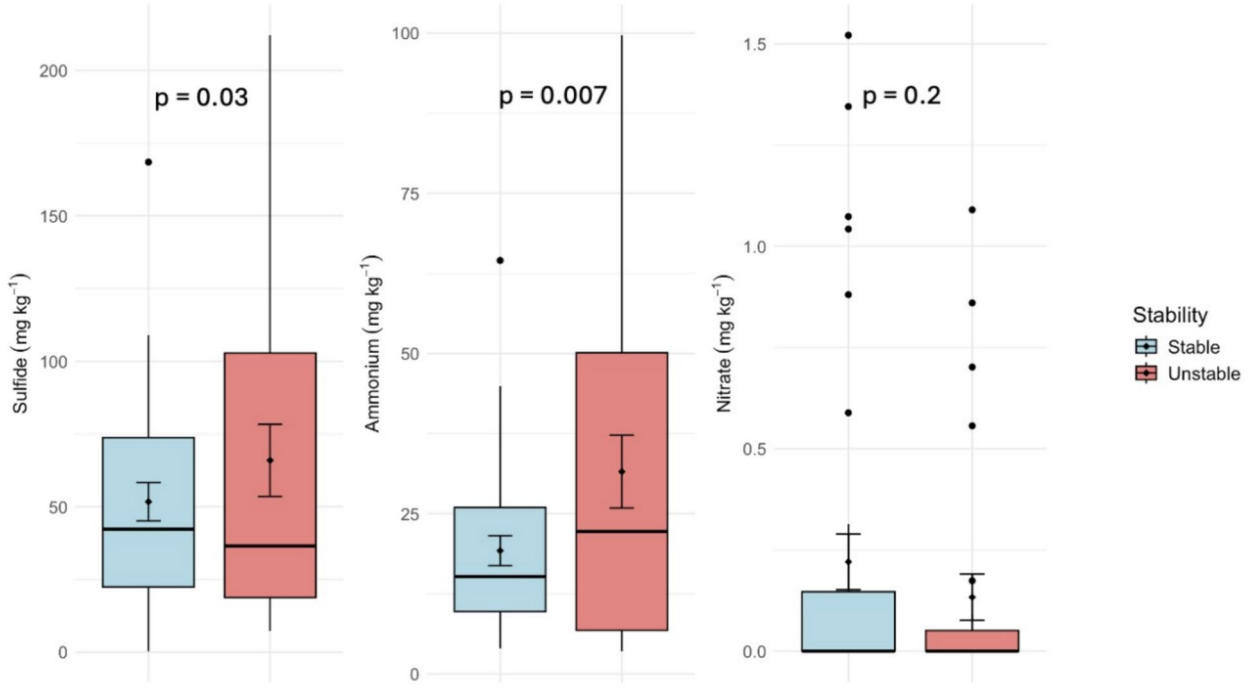

Fig. 2 Boxplots comparing stable and unstable soil for NH_4^+, sulfide, and NO_3^-. The boxes represent the interquartile range, and the lines in the boxes are the median. Dots inside the boxes represent mean values, and bars represent standard error

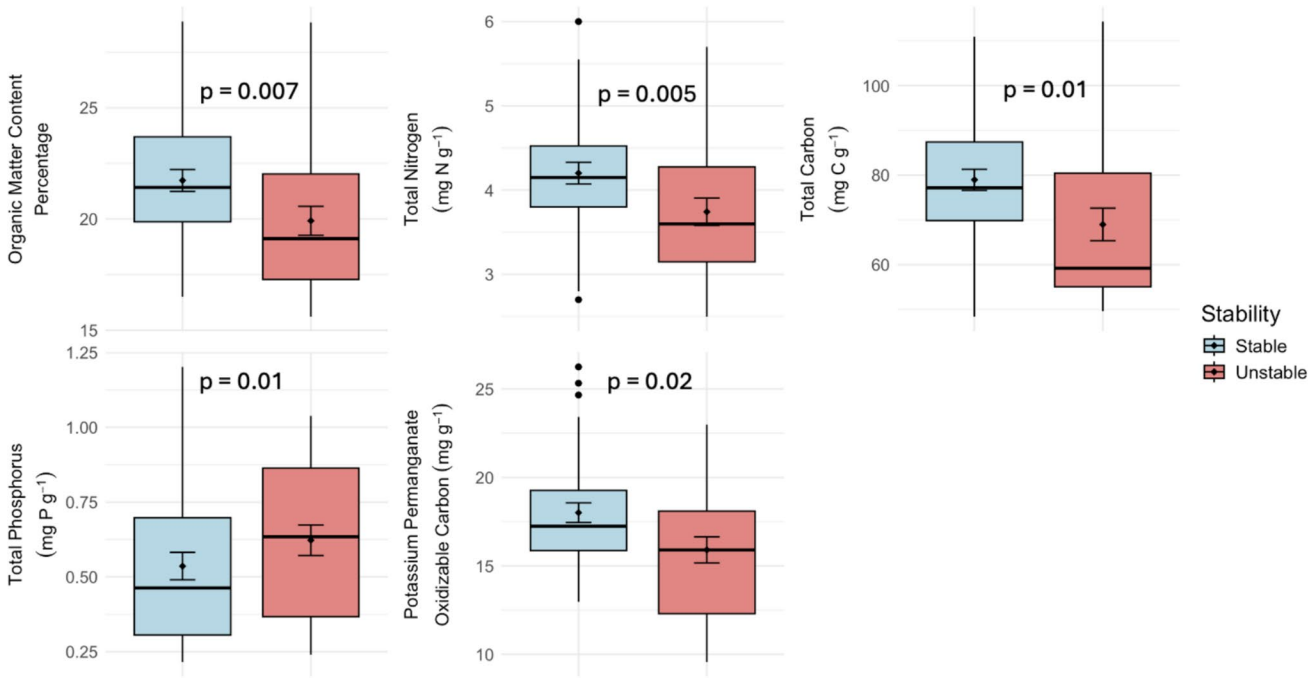

Fig. 3 Boxplots comparing stable and unstable soil for OM content, TN, TC, TP, and POXC. The boxes represent the interquartile range, and the lines in the boxes are the median. Dots inside the boxes represent mean values, and bars represent standard error

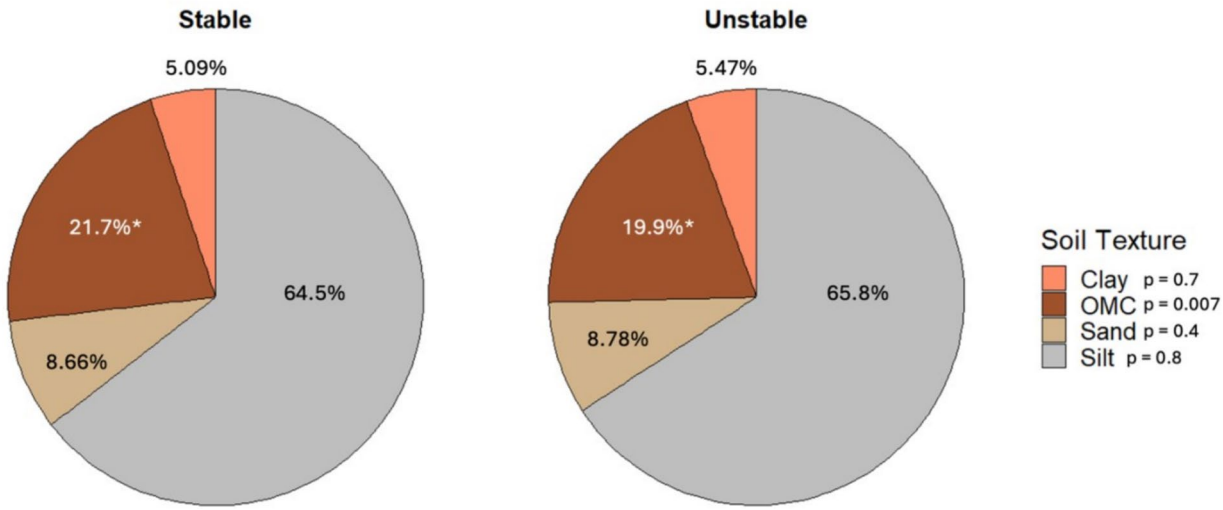

Fig. 4 Pie charts comparing the mean distribution of clay, silt, sand, and organic matter content from stable and unstable soil. The symbol "*" indicates statistically significant results in the graph. OMC is the only statistically significant result

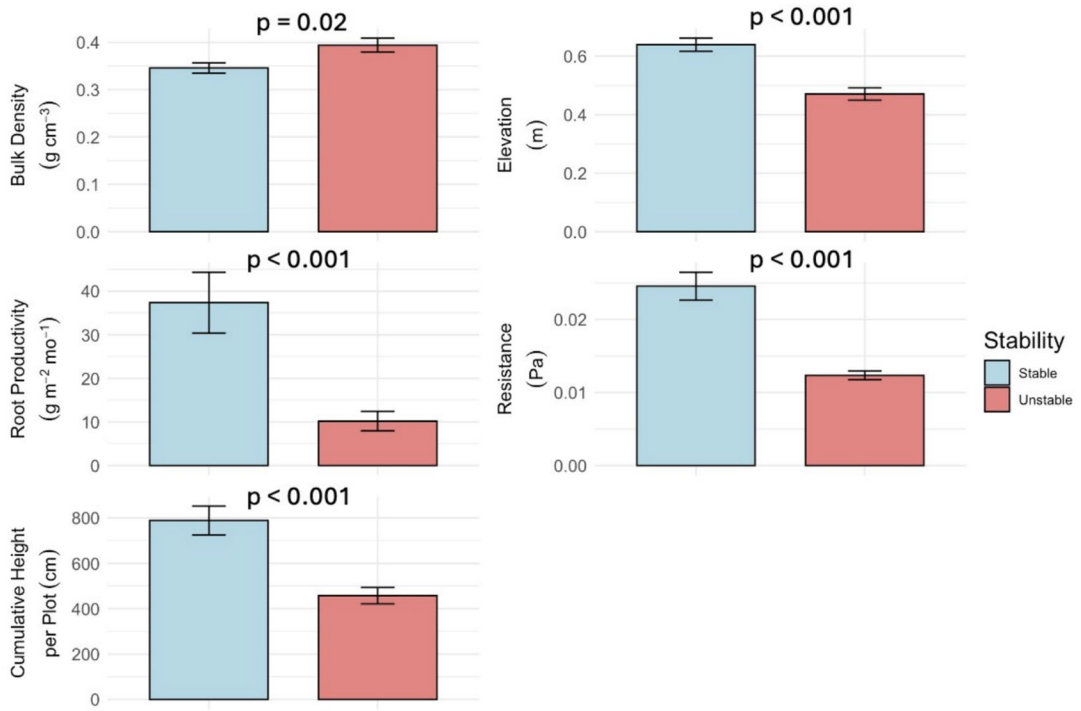

Fig. 5 Bar plots comparing stable and unstable soil for BD, elevation, root productivity, and resistance. The top of the bars represents the mean, and brackets represent the standard error

in wetlands, and that just 2–3 weeks of dry-down can significantly and permanently reduce floc thickness by ~ 60% and enhance soil consolidation (Boudreau et al., 2024). Similarly, soils with improved drainage are more consolidated and less prone to collapse (Day et al., 2011). Effective drainage, including the marsh platform being at the appropriate elevation relative to the tidal frame in coastal wetlands, can reduce ponding, maintain adequate tidal flushing, and subsequently enhance plant growth and C sequestration (Mendelssohn & Seneca, 1980; Snedden et al., 2015). Because this was an observational study, the direction of a causal relationship between elevation and plant and soil properties could not be empirically determined. However, it was noted in the field that many of the unstable soils were located near

tidal creeks experiencing headward expansion, a process that occurs when vertical accretion cannot keep pace with rising sea levels and causes shallow subsidence and an expansion in the density and length of the drainage network (Hughes et al., 2009). As with previous coastal marsh studies in South Carolina, these creek head areas were characterized by low belowground biomass and low soil strength (Wilson et al., 2022). In some cases, the physical barrier created by the oyster berms was the only thing impeding the drainage creeks from connecting with the main channel of the river. Based on these observations, it is hypothesized that the lower elevation is driving plant and soil properties, which may subsequently feedback into greater elevation change. A study conducted on blackwater marshes in Chesapeake Bay argued marshes can retain elevation through organic matter accumulation and sediment trapping, but when tidal channels widen through wave erosion and ponds deepen past a critical threshold, natural recovery of the marsh becomes unlikely due to high inundation (Schepers et al., 2020).

Soil and Plant Physicochemical Parameters Differed by Stability

Land managers in the GTMNERR visually assess their land, and they have observed increased unvegetated salt marsh areas (Endris et al., 2023). This study utilized qualitative observations, like visual vegetation density and tactile soil consolidation, to select stable and unstable plots, which were then sampled and analyzed in a lab to quantify physicochemical differences. Results indicate these visual and tactile cues of marsh degradation can be a reliable way to predict soil biogeochemical properties in the GTMNERR as observable differences between stable and unstable soil in the field were correlated with quantitative biogeochemical differences in a lab. Specifically, NH_4^+, S^{2-}, OM content, total C, and total N differed significantly based on visual/tactile characterization. Unstable soils averaged 64% higher NH_4^+, 28% higher S^{2-}, and 19% higher total P than stable soils. Visually, increased inundation, which was observed as standing water during low tide, and lower *S. alterniflorus* abundance could indicate higher NH_4^+ concentrations in the soil, a potential product of more anaerobic environments and less plant uptake (Mendelssohn & Seneca, 1980; Morris, 1980). *S. alterniflorus* utilizes NH_4^+ for its growth, but persistently waterlogged soil can limit this uptake. Studies have shown that shorter versions of *S. alterniflorus* are found in more waterlogged soils, in tandem with higher concentrations of unassimilated NH_4^+ in the soil (Mendelssohn, 1979a, 1979b). Alcoholic fermentation is an energy pathway utilized by wetland plants, but higher S^{2-} concentrations (as found in the unstable soils) can stress *S. alterniflorus* by suppressing alcohol dehydrogenase, an enzyme involved in this pathway (Koch et al., 1990). Sulfide toxicity has been associated with less adenosine monophosphate, adenosine diphosphate, and adenosine triphosphate (ATP) in *S. alterniflorus* roots, limiting N uptake (Koch et al., 1990).

Soil OM is produced and stored by plants in place or deposited by floodwater; OM is the primary source of C and N in most wetland soils (Naidu et al., 2022). Higher plant biomass in the stable plots likely provided more OM from plant litter and live and dead roots, while also releasing POXC into the soil (Bot & Benites, 2005). A study conducted in Jiangsu Yancheng Wetland National Nature Reserve in China found that *Sporobolus alterniflorus* invasion was a strong source of soil OM and N (Yang, et al., 2016). Strongly correlated with OM, total C, and total N in wetland soils, POXC is a portion of the organic C pool that is semi-labile (Chambers et al., 2024). Stable soils averaged 10% higher OM, 15% higher total C, 12% higher total N, and 13% higher POXC than unstable soils. Moreover, our study also found 267% higher root productivity (belowground biomass) in stable soil. Positive correlations have been found by other researchers between live belowground biomass, increased soil strength, and wetland shelf stabilization (Brooks et al., 2021; Chen et al., 2012; Nyman et al., 1994; Sasser et al., 2018; Turner, 2011). Therefore, if elevated levels of S^{2-} in unstable soil caused root stress and less NH_4^+ uptake of *Sporobolus alterniflorus*, then the lower plant cover in the unstable plots was likely responsible for the lower total C, N, and root productivity in these soils (Figs. 3 and 5).

Particle size distribution and soil compaction represent physical factors in the soil which interact with the hydrologic conditions. Higher clay and silt content is associated with higher moisture retaining capacity, while higher sand content is associated with higher rates of water conveyance through the soil (Giap et al., 2021). Although it was theorized the inability of the unstable soils to support weight was related to a higher proportion of fines (silt and clay particles), the evidence did not support differences in soil particle size distribution as a factor of stability. Soil BD was 11% higher in unstable plots, likely due to the negative correlation between BD and OM content, the latter of which was higher in stable plots (Hossain et al., 2015).

Link Between Dead Oyster Berms and Marsh Stability Remains Uncertain

Potential causes of marsh degradation in the GTMNERR have been anecdotally attributed to sea level rise and/or the large mounds of dead oyster rake from boat wakes built between the river and marsh front, which have been viewed as an impediment to wetland flushing by altering tidal creek flow (Bacopoulos et al., 2019; Dix et al., 2021; Endris et al., 2023; Price, 2006). As sea level rises and pushes more sulfate-containing seawater further into coastal wetlands for

longer periods of time, porewater S^{2-} concentrations can increase (Leyden et al., 2023), which could lead to plant root mortality and lower productivity (Koch et al., 1990). A similar study was conducted in the Great Bay Estuary (New England, USA) on how human-made barriers impacted tidal marshes. Where the earthen berm restricted tidal drainage, there were high sulfide and salinity concentrations and less plant cover, and where the berm restricted tidal flooding, there was less organic matter (Mora & Burdick, 2013). These previous findings suggest the dead oyster rakes at the GTMNERR may similarly be a hydrologic obstruction causing the observed high soil sulfide and lower plant cover in the unstable soils. However, in the GTMNERR, both stable and unstable plots were identified behind the same oyster rake, suggesting this alone cannot be the cause of the heterogeneous patchwork of stable and unstable wetland. Furthermore, the overwhelming presence of oyster rakes within the study region made it unfeasible to test sites without rakes, so we are unable to make conclusions about the contributions of the rakes themselves in inhibiting tidal exchange or contributing to marsh deterioration. Future research should investigate the potential role of the expanding tidal creek network behind the rakes in contributing to the observed patchwork of stability. A study conducted in the GTMNERR on the effect of sea level rise on salt marshes using a tide-marsh equilibrium model predicted that areas of salt marsh located near tidal creeks will turn into open water areas, and marshes located away from tidal creeks will be able to migrate to undeveloped areas and survive sea level rise (Bacopoulos et al., 2019).

Physiochemical Properties Varied by Site and Soil Depth

While the goal of this study was to investigate differences between stable and unstable plots, there were also notable differences between sites. Based on the extractable nutrient data, a nutrient gradient appears to exist along the river, whereby soil nutrients were generally higher at northern sites than at southern sites, particularly NO_3^- and SRP. Since the southern sites are closer in proximity to the Atlantic Ocean, this gradient may result from the dilution of nutrient-enriched river water (which drains a partially developed watershed) mixing with lower nutrient ocean water. A progressive decline in elevation was also notable when moving downstream, in addition to within-site differences based on stability.

Depending on site, the differences between stable and unstable plots varied in magnitude, and this variability is still not well understood. Many of the site-scale differences may have a geologic origin. For example, Site 3 was identified as the stable end member site with no unstable soils evident. Site 3 also had higher sand content than other sites, so it may exist at a location of historic river deposition. Meanwhile, other sites may be located on areas of the river historically characterized by erosion and incision. As mentioned above, proximity to tidal creeks may also explain different degrees of stability. A report by Endris et al. (2023) utilized Geographic Information Systems to evaluate early charts, historic aerials, and elevation maps that included the study area. These historic maps and images suggest the conversion of significant areas of vegetated tidal wetlands into unvegetated mudflats between 1860 and 2023, particularly in areas of close proximity to tidal creeks. This loss of vegetated wetland co-occurred with a 5% decrease in the elevation of tidal wetlands along the Tolomato River between 1860 and 2015 (Endris et al., 2023). Another study utilizing a Hydro-MEM model suggested most of the study regions' tidal marshes are vulnerable to sea level rise and at risk of conversion to open water, especially areas located closer to tidal creeks (Bacopoulos et al., 2019). Finally, in addition to sea level rise induced submergence, erosion from high wave energy (like boat wakes) can also lead to open mudflat areas (Price, 2006). Therefore, geomorphic location, the historical erosional or depositional character of each site, and the plot-level proximity to tidal creeks are likely coalescing to interact with sea level rise and erosion stressors. This has created a patchwork of marsh vulnerability in this region that requires further investigation, particularly studies leveraging additional historic and remote sensing data, as well as hydrology and sediment dynamics research.

Many soil parameters (e.g., NO_3^-, OMC, DOC, TN, and TP) generally decreased in concentration as soil depth increased, and BD and sulfide generally increased in depth. Nitrate, an oxidized form of inorganic N, likely decreased with depth as the soil became more anaerobic, while OMC, DOC, and TN may have decreased due to higher input of plant litter at the upper layers of soil (Reddy & DeLaune, 2008; Bot & Benites, 2005). Bulk density presented inverse results because as OM content decreases, generally BD increases (Hossain et al., 2015). Total P may have decreased with depth from binding to elements in the soil like ferric iron, calcium, aluminum, and clay under more anaerobic conditions (Mitsch & Gosselink, 2015). Finally, sulfide likely increased with depth due to increased anaerobic conditions where sulfate reduction would be more likely to occur (Koch et al., 1990).

Conclusion

We hypothesized that unstable plots would exhibit higher NH_4^+, S^{2-}, OMC, POXC, clay, and silt, and lower NO_3^-, sand, root productivity, elevation, and soil resistance compared to stable plots. Our study supported NH_4^+ and S^{2-} being higher in unstable plots, but OMC and POXC were

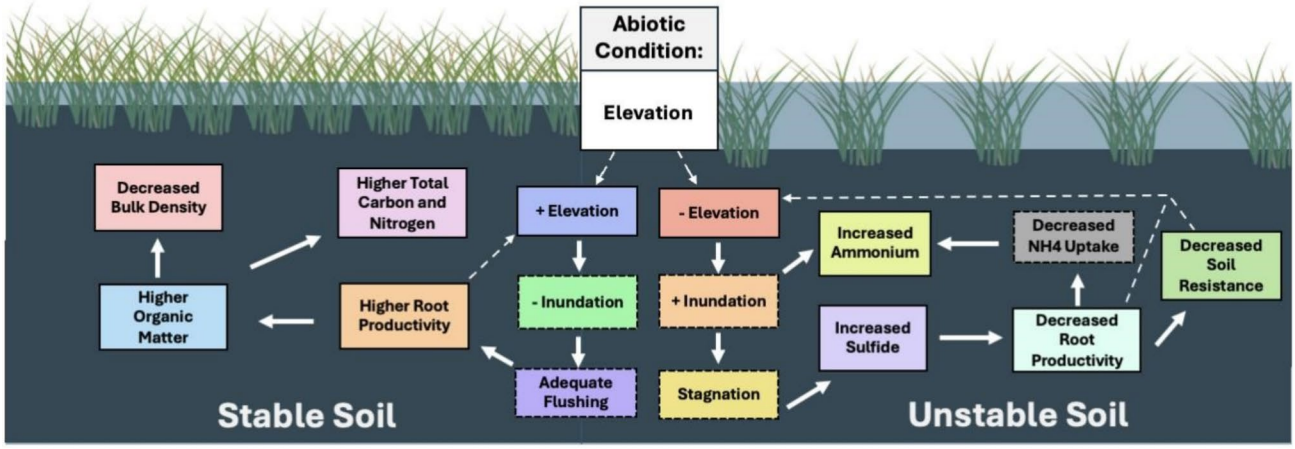

Fig. 6 Hypothetical flow chart of empirical soil and plant relationships and perceived causation based on previous research. Dashed lines around the boxes were inferred, and solid lines around the boxes were quantified. Dashed arrows indicate possible feedback loops to elevation differences

lower in unstable plots. Root productivity, elevation, and soil resistance were lower in unstable plots, which also supports our hypotheses. Clay, silt, sand, and NO_3^- exhibited no differences between stable and unstable plots. Results indicate the strongest correlation (using a Pearson correlation) for the difference between stable and unstable plots was seen with elevation, resistance, belowground biomass, and cumulative plant height, which we predict to be drivers of the observed soil properties (Fig. 6).

Overall, our data suggest the lower elevation in unstable soil is likely leading to increased inundation (and decreased tidal flushing), which may cause sulfide accumulation (Koch et al., 1990; Morris, 1980; Fig. 6). Furthermore, sulfide is known to stress *S. alterniflorus* roots (Lamers et al., 2013; Koch et al., 1990; Morris, 1980), which may be the cause of lower root productivity in the unstable soils of this study. *S. alterniflorus* utilizes NH_4^+ as a nutrient (Morris, 1980; Morris, 1984; Hessini et al., 2017; Lamba et al., 2017), but sulfide may reduce its uptake by suppressing an enzyme involved in alcoholic fermentation (Koch et al., 1990), thus increasing unassimilated NH_4^+ in unstable soil. Finally, *S. alterniflorus* is likely the primary contributor of OMC (and thus also C and N) into the soil. Plant stress, leading to less plant biomass in unstable soil, would therefore lead to the observed lower concentrations of C and N in unstable soil, relative to stable soil.

These findings offer strong support for using qualitative visual (sparse vegetation and pockets of open water) and tactile (soupy, unsupportive soils) indicators to identify differences in plant and soil properties. This provides immediate information to land managers for an improved understanding of the ecological properties and processes underlying rapid landscape-scale changes. For example, the marsh area in this study showed decreased vegetation in aerial imagery from 1860 to 2023, which could be due to boat wake energy eroding and destabilizing *S. alterniflorus* (Endris et al., 2023; Price, 2006). Boat wakes have also been correlated with increased dead oyster berm along the Atlantic Intercoastal Waterway, a unique feature of this region (Grizzle et al., 2002). This erosion could lead to less plant biomass, less OM content from less plant turnover, lower accretion rates, which could lead to lower elevation, and increased inundation and sulfide accumulation from increased low-lying areas. This work also lays the foundation for further experimental research to disentangle the sequence of cause-and-effect relationships that would inform what actions or interventions may be appropriate for ecosystem management or restoration.

Acknowledgements The authors recognize the generous time and support from Nikki Dix, Lia Thompson, Kaitlyn Diez, Alex North, Shannon Brew, Sara Gay, Anthony Mirabito, Naija Cheek, Nathan Swinburne, Mercedes Pinzon, Megan Jensik, Avalon Ramsey, Lucas Vivas, Alexis Pellegrino, Nicole Boisson, Jesus Villavisanis, Mumtahina Riza, Tess Adgie, Morgan Mack, Jocelyn Bravo, Michelle Moczulski, Aaron Freeman, and Scott Jones, who all contributed to the completion of this work.

Author Contribution Jennifer Volk collected soil data, analyzed it in the lab, performed statistics on the data, created graphs in paper, and wrote most of the manuscript.

Cathilyn L. McIntosh collected vegetation data, analyzed it in the lab, and helped write a large part of the manuscript.

Adam Langley, Samantha K. Chapman, and Lisa G. Chambers all helped fund the research, guided Jennifer and Cathilyn on the research, and made edits to the manuscript.

Funding The authors gratefully acknowledge funding from the Friends of the Guana Tolomato Matanzas National Estuarine Research Reserve

and the National Science Foundation Division of Environmental Biology (Award #2225000), which supported this research.

Data Availability The datasets generated during the current study are not publicly available as they have not been made publicly accessible yet but are available from the corresponding author on reasonable request.

Declarations

Ethics Approval and Consent to Participate Not applicable.

Consent for Publication Not applicable

Competing Interests The authors declare no competing interests.

References

Almuktar, S. A. A. A. N., Abed, S. N., & Scholz, M. (2018). Wetlands for wastewater treatment and subsequent recycling of treated effluent: A review. *Environmental Science and Pollution Research, 25*(24), 23595–23623. https://doi.org/10.1007/s11356-018-2629-3

Andersen, J. M. (1976). An ignition method for determination of total phosphorus in lake sediments. *Water Research, 10*(4), 329–331. https://doi.org/10.1016/0043-1354(76)90175-5

Bacopoulos, P., Tritinger, A. S., & Dix, N. G. (2019). Sea-level rise impact on salt marsh sustainability and migration for a subtropical estuary: GTMNERR (Guana Tolomato Matanzas National Estuarine Research Reserve). *Environmental Modeling & Assessment, 24*(2), 163–184. https://doi.org/10.1007/s10666-018-9622-6

Barbier, E. B. (2013). Valuing ecosystem services for coastal wetland protection and restoration: Progress and challenges. *Resources,2*(3), Article Article 3. https://doi.org/10.3390/resources2030213

Bennett, J. D., & Chambers, L. (2023). Wetland soil carbon storage exceeds uplands in an urban natural area (Florida, USA). *Soil Research, 61*(6), 542–559. https://doi.org/10.1071/SR22235

Bertolini, C., & da Mosto, J. (2021). Restoring for the climate: A review of coastal wetland restoration research in the last 30 years. *Restoration Ecology*. https://doi.org/10.1111/rec.13438

Bhadha, J., Khatiwada, R., Galindo, S., Xu, N., & Capasso, J. (2018). Evidence of soil health benefits of flooded rice compared to fallow practice. *Sustainable Agriculture Research, 7*, 31. https://doi.org/10.5539/sar.v7n4p31

Bot, A., & Benites, J. (2005). *The importance of soil organic matter*. Food and Agriculture Organization of the United Nations. Retrieved June 6, 2024, from https://www.fao.org/3/a0100e/a0100e00.htm#Contents

Boudreau, P., Sees, M., Mirabito, A. J., & Chambers, L. G. (2024). Utilizing water level drawdown to remove excess organic matter in a constructed treatment wetland. *Science of the Total Environment, 918*, Article 170508. https://doi.org/10.1016/j.scitotenv.2024.170508

Breithaupt, J. L., Steinmuller, H. E., Rovai, A. S., Engelbert, K. M., Smoak, J. M., Chambers, L. G., Radabaugh, K. R., Moyer, R. P., Chappel, A., Vaughn, D. R., Bianchi, T. S., Twilley, R. R., Pagliosa, P., Cifuentes-Jara, M., & Torres, D. (2023). An improved framework for estimating organic carbon content of mangrove soils using loss-on-ignition and coastal environmental setting. *Wetlands, 43*(6), 57. https://doi.org/10.1007/s13157-023-01698-z

Brooks, H., Möller, I., Carr, S., et al. (2021). Resistance of salt marsh substrates to near-instantaneous hydrodynamic forcing. *Earth Surface Processes and Landforms,46*, 67–88. https://doi.org/10.1002/esp.4912

Cahoon, D. R. (2015). Estimating relative sea-level rise and submergence potential at a coastal wetland. *Estuaries and Coasts, 38*(3), 1077–1084.

Cahoon, D. R., Lynch, J. C., Roman, C. T., Schmit, J. P., & Skidds, D. E. (2019). Evaluating the relationship among wetland vertical development, elevation capital, sea-level rise, and tidal marsh sustainability. *Estuaries and Coasts, 42*(1), 1–15. https://doi.org/10.1007/s12237-018-0448-x

Cahoon, D. R., McKee, K. L., & Morris, J. T. (2021). How plants influence resilience of salt marsh and mangrove wetlands to sea-level rise. *Estuaries and Coasts, 44*, 883–898. https://doi.org/10.1007/s12237-020-00834-w

Castañeda-Moya, E., Twilley, R. R., & Rivera-Monroy, V. H. (2013). Allocation of biomass and net primary productivity of mangrove forests along environmental gradients in the Florida Coastal Everglades, USA. *Forest Ecology and Management, 307*, 226–241. https://doi.org/10.1016/j.foreco.2013.07.011

Chambers, L. G., Mirabito, A. J., Brew, S., Nitsch, C. K., Bhadha, J. H., Hurst, N. R., & Berkowitz, J. F. (2024). Evaluating permanganate oxidizable carbon (POXC)'s potential for differentiating carbon pools in wetland soils. *Ecological Indicators, 167*, Article 112624. https://doi.org/10.1016/j.ecolind.2024.112624

Chambers, L. G., Steinmuller, H. E., & Breithaupt, J. L. (2019). Toward a mechanistic understanding of "peat collapse" and its potential contribution to coastal wetland loss. *Ecology*. https://doi.org/10.1002/ecy.2720

Chen, Y., Thompson, C. E. L., & Collins, M. B. (2012). Saltmarsh creek bank stability: Biostabilisation and consolidation with depth. *Continental Shelf Research, 35*, 64–74. https://doi.org/10.1016/j.csr.2011.12.009

Clark, M., Greco, S., & Curry, S. (2010). *Wetlands in your county: Alachua*. EDIS Publication SL 307. Retrieved May 8, 2024, from http://edis.ifas.ufl.edu

Culman, S., Hurisso, T., & Wade, J. (2021). Permanganate oxidizable carbon: An indicator of biologically-active soil carbon In D. L. Karlen, D. E. Scott, & M. M. Mikha (Eds.), *Soil Health Series: Volume 2 Laboratory Methods for Soil Health Analysis* (pp. 152–175). ASA, CSSA, and SSSA Books.

Davidson, N. (2014). How much wetland has the world lost? Long-term and recent trends in global wetland area. *Marine and Freshwater Research, 65*, 936–941. https://doi.org/10.1071/MF14173

Day, J. W., Kemp, G. P., Reed, D. J., Cahoon, D. R., Boumans, R. M., Suhayda, J. M., & Gambrell, R. (2011). Vegetation death and rapid loss of surface elevation in two contrasting Mississippi delta salt marshes: The role of sedimentation, autocompaction and sea-level rise. *Ecological Engineering, 37*(2), 229–240. https://doi.org/10.1016/j.ecoleng.2010.11.021

Deegan, L., Johnson, D. S., Warren, R. S., Peterson, B., Fleeger, J. W., Fagherazzi, S., & Wollheim, W. (2012). Coastal eutrophication as a driver of marsh loss. *Nature,490*(7420), 388–392.

Deng, Y., et al. (2022). Assessing and characterizing carbon storage in wetlands of the Guangdong– Hong Kong–Macau Greater Bay Area, China, during 1995–2020. *IEEE Journal of Selected Topics in Applied Earth Observations and Remote Sensing,15*, 6110–6120. https://doi.org/10.1109/JSTARS.2022.3192267

Dix, N., Brockmeyer, R., Johns, S., Water, R., District, M., Chapman, S., Angelini, C., Kidd, S., Eastman, S., Radabaugh, K.R. & Moyer, R.P. (2021). Chapter 13 Northeast Florida. In K. R. Radabaugh & R.P. Moyer (Eds.), *Coastal Habitat Integrated Mapping and Monitoring Program Report for the State of Florida No. 2*. Retrieved January 8, 2025, from https://myfwc.com/media/26620/chimmpv2-ch13.pdf

Endris C., Shull S., Woolfolk A., Brophy L. S., Brumbaugh D. R., Crooks J., Haines D., Fuller R., Reinl K., Sanger D., Stevens R., &

Wasson K. (2023). *Estuarine habitats in and around GTM NERR, Florida: Past, present, and future*. National Estuarine Research Reserve System and the Institute for Applied Ecology. Retrieved May 28, 2025, from https://www.nerra.org/estuary-change

Frazel, D. (2009). *Site profile of the Guana Tolomato Matanzas National Estuarine Research Reserve*. Retrieved February 24, 2024, from https://coast.noaa.gov/data/docs/nerrs/Reserves_GTM_SiteProfile.pdf

Giap, G. E., Rudiyanto, & Sulaiman, M. S. (2021). Water infiltration into sand, silt, and clay at field capacity. *Journal of Advanced Research in Fluid Mechanics and Thermal Sciences*, *84*(2), Article 2. https://doi.org/10.37934/arfmts.84.2.159166

Grizzle, R., Adams, J., & Walters, L. (2002). Historical changes in intertidal oyster (Crassostrea virginica) reefs in a Florida lagoon potentially related to boating activities. *Journal of Shellfish Research*. Retrieved November 7, 2016, from https://scholars.unh.edu/jel/294

Haag, K. H., & Lee, T. M. (2010). Hydrology and ecology of freshwater wetlands in Central Florida—A primer. In *Circular* (1342). U.S. Geological Survey. https://doi.org/10.3133/cir1342

Harttung, S. A., Radabaugh, K. R., Moyer, R. P., Smoak, J. M., & Chambers, L. G. (2021). Coastal riverine wetland biogeochemistry follows soil organic matter distribution along a marsh-to-mangrove gradient (Florida, USA). *Science of The Total Environment, 797*,149056. https://doi.org/10.1016/j.scitotenv.2021.149056

Hessini, K., Kronzucker, H. J., Abdelly, C., & Cruz, C. (2017). Drought stress obliterates the preference for ammonium as an N source in the C4 plant *Sporobolus alterniflorus*. *Journal of Plant Physiology, 213*, 98–107. https://doi.org/10.1016/j.jplph.2017.03.003

Ho, J., & Chambers, L. G. (2020). Willow-shrub encroachment affects physicochemical properties differently in two subtropical freshwater marshes. *Wetlands Ecology and Management,28*(2), 389–395. https://doi.org/10.1007/s11273-019-09705-z

Hossain, M. F., Chen, W., & Zhang, Y. (2015). Bulk density of mineral and organic soils in the Canada's arctic and sub-arctic. *Information Processing in Agriculture,2*(3), 183–190. https://doi.org/10.1016/j.inpa.2015.09.001

Hughes, Z. J., FitzGerald, D. M., Wilson, C. A., Pennings, S. C., Więski, K., & Mahadevan, A. (2009). Rapid headward erosion of marsh creeks in response to relative sea level rise. *Geophysical Research Letters*. https://doi.org/10.1029/2008GL036000

Kennish, M. J. (2001). Coastal salt marsh systems in the U.S.: A review of anthropogenic impacts. *Journal of Coastal Research*, *17*(3), 731–748.

Koch, M. S., Mendelssohn, I. A., & McKee, K. L. (1990). Mechanism for the hydrogen sulfide-induced growth limitation in wetland macrophytes. *Limnology and Oceanography,35*(2), 399–408. https://doi.org/10.4319/lo.1990.35.2.0399

Lamba, S., Bera, S., Rashid, M., Medvinsky, A. B., Sun, G.-Q., Acquisti, C., Chakraborty, A., & Li, B.-L. (2017). Organization of biogeochemical nitrogen pathways with switch-like adjustment in fluctuating soil redox conditions. *Royal Society Open Science, 4*(1), Article 160768. https://doi.org/10.1098/rsos.160768

Lamers, L. P., Govers, L. L., Janssen, I. C., Geurts, J. J., Van der Welle, M. E., Van Katwijk, M. M., Van der Heide, T., Roelofs, J. G., & Smolders, A. J. (2013). Sulfide as a soil phytotoxin—A review. *Frontiers in Plant Science*, *4*. https://www.frontiersin.org/journals/plant-science/articleshttps://doi.org/10.3389/fpls.2013.00268

Langley, J. A., McKee, K. L., Cahoon, D. R., Cherry, J. A., & Megonigal, J. P. (2009). Elevated CO2 stimulates marsh elevation gain, counterbalancing sea-level rise. *Proceedings of the National Academy of Sciences of the United States of America,106*(15), 6182–6186.

Leyden, E., Farkaš, J., Hutson, J., & Mosley, L. M. (2023). Controls on sulfide accumulation in coastal soils during simulated sea level rise. *Geochimica Et Cosmochimica Acta, 347*, 88–101. https://doi.org/10.1016/j.gca.2023.02.018

McKee, K. L., Mendelssohn, I. A., & Hester, M. W. (1988). Reexamination of pore water sulfide concentrations and redox potentials near the aerial roots of *Rhizophora mangle* and *Avicennia germinans*. *American Journal of Botany,75*(9), 1352–1359. https://doi.org/10.1002/j.1537-2197.1988.tb14196.x

Mendelssohn, I. A. (1979a). The influence of nitrogen level, form, and application method on the growth response of *Spartina alterniflora* in North Carolina. *Estuaries,2*(2), 106–112. https://doi.org/10.2307/1351634

Mendelssohn, I. A. (1979b). Nitrogen metabolism in the height forms of Spartina alterniflora in North Carolina. *Ecology, 60*(3), 574–584. https://doi.org/10.2307/1936078

Mendelssohn, I. A., & Seneca, E. D. (1980). The influence of soil drainage on the growth of salt marsh cordgrass Spartina alterniflora in North Carolina. *Estuarine and Coastal Marine Science, 11*, 27–40. https://doi.org/10.1016/S0302-3524(80)80027-2

Minasny, B. (2012). Contrasting soil penetration resistance values acquired from dynamic and motor-operated penetrometers. *Geoderma, 177–178*, 57–62. https://doi.org/10.1016/j.geoderma.2012.01.026

Mitsch, W., & Gosselink, J. (2015). *Wetlands, 5th Edition*. John Wiley & Sons.

Mora, J. W., & Burdick, D. M. (2013). The impact of man-made earthen barriers on the physical structure of New England tidal marshes (USA). *Wetlands Ecology and Management, 21*(6), 387–398. https://doi.org/10.1007/s11273-013-9309-3

Morris, J. T. (1980). The nitrogen uptake kinetics of Sporobolus alterniflorus in culture. *Ecology, 61*(5), 1114–1121. https://doi.org/10.2307/1936831

Morris, J. T. (1984). Effects of oxygen and salinity on ammonium uptake by *Sporobolus alterniflorus* Loisel. And *Spartina patens* (Aiton) Muhl. *Journal of Experimental Marine Biology and Ecology*, *78*(1), 87–98. https://doi.org/10.1016/0022-0981(84)90071-6

Morris, J. T., Sundareshwar, P. V., Nietch, P. T., Kjerfve, B., & Cahoon, D. R. (2002). Responses of coastal wetlands to rising sea levels. *Ecology,83*(10), 2869–2877.

Moseman-Valtierra, S., Abdul-Aziz, O. I., Tang, J., et al. (2016). Carbon dioxide fluxes reflect plant zonation and belowground biomass in a coastal marsh. *Ecosphere, 7*, Article e01560. https://doi.org/10.1002/ecs2.1560

Naidu, S. A., Kathiresan, K., Simonson, J. H., Blanchard, A. L., Sanders, C. J., Pérez, A., Post, R. M., Subramoniam, T., Naidu, R. A., & Narender, R. (2022). Carbon and nitrogen contents driven by organic matter source within Pichavaram wetland sediments. *Journal of Marine Science and Engineering,10*(1), Article Article 1. https://doi.org/10.3390/jmse10010053

NOAA. (2024). *National Estuarine Research Reserve System*. Guana Tolomato Matanzas National Estuarine Research Reserve. Retrieved June 16, 2024, from https://coast.noaa.gov/nerrs/reserves/gtm.html

Nyman, J. A., Carloss, M., Delaune, R. D., & Patrick, W. H. (1994). Erosion rather than plant dieback as the mechanism of marsh loss in an estuarine marsh. *Earth Surface Processes and Landforms, 19*, 69–84. https://doi.org/10.1002/esp.3290190106

Orson, R. A., Panageotou, W., & Leatherman, S. P. (1985). Response of tidal salt marshes of the US Atlantic and Gulf coasts to rising sea levels. *Journal of Coastal Research, 1*, 29–37.

Parkinson, R. W., & Wdowinski, S. (2022). Accelerating sea-level rise and the fate of mangrove plant communities in South Florida, U.S.A. *Geomorphology,412*, Article 108329.

Price, F. D. (2006). *Quantification, analysis, and management of intracoastal waterway channel margin erosion in the Guana Tolomato*

Matanzas National Estuarine Research Reserve, Florida (Technical Report No. 1). Retrieved January 8, 2025, from https://coast.noaa.gov/data/docs/nerrs/Research_TechSeries_TechSeries200601.pdf

Raposa, K., Wasson, K., Smith, E., Crooks, J., Delgado, P., Fernald, S., Ferner, M., Helms, A., Hice, L., Mora, J., Puckett, B., Sanger, D., Shull, S., Spurrier, L., Stevens, R., & Lerberg, S. (2016). Assessing tidal marsh resilience to sea-level rise at broad geographic scales with multi-metric indices. *Biological Conservation,204*, 263–275.

Reddy, R., & DeLaune, R. (2008). *Biogeochemistry of Wetlands: Science and Applications*. New York: CRC Press.

Reed, D. J. (1995). The response of coastal marshes to sea-level rise: Survival or submergence. *Earth Surface Processes and Landforms,20*(1), 39–48.

Sanglerat, G. (1972). *The penetrometer and soil exploration*. Elsevier Science.

Sasser, C. E., Evers-Hebert, E., Holm, G. O., Milan, B., Sasser, J. B., Peterson, E. F., & DeLaune, R. D. (2018). Relationships of marsh soil strength to belowground vegetation biomass in Louisiana coastal marshes. *Wetlands, 38*, 401–409.

Schepers, L., Brennand, P., Kirwan, M. L., Guntenspergen, G. R., & Temmerman, S. (2020). Coastal marsh degradation into ponds induces irreversible elevation loss relative to sea level in a microtidal system. *Geophysical Research Letters,47*(18), Article e2020GL089121. https://doi.org/10.1029/2020GL089121

Snedden, G. A., Cretini, K., & Patton, B. (2015). Inundation and salinity impacts to above- and belowground productivity in *Spartina patens* and *Spartina alterniflora* in the Mississippi 37 River deltaic plain: Implications for using river diversions as restoration tools. *Ecological Engineering,81*, 133–139. https://doi.org/10.1016/j.ecoleng.2015.04.035

Steinmuller, H. E., Foster, T. E., Boudreau, P., Hinkle, C. R., & Chambers, L. G. (2020). Characterization of herbaceous encroachment on soil biogeochemical cycling within a coastal marsh. *Science of the Total Environment, 738*, Article 139532. https://doi.org/10.1016/j.scitotenv.2020.139532

Turner, R. E. (2011). Beneath the salt marsh canopy: Loss of soil strength with increasing nutrient loads. *Estuaries and Coasts, 34*, 1084–1093. https://doi.org/10.1007/s12237-010-9341-y

Twohig, T. M., & Stolt, M. H. (2011). Soils-based rapid assessment for quantifying changes in salt marsh condition as a result of hydrologic alteration. *Wetlands, 31*, 955–963. https://doi.org/10.1007/s13157-011-0210-7

Vincent, R. E., Burdick, D. M., & Dionne, M. (2013). Ditching and ditch-plugging in New England salt marshes: Effects on hydrology, elevation, and soil characteristics. *Estuaries and Coasts, 36*, 610–625. https://doi.org/10.1007/s12237-012-9583-y

Wang, X., Wang, L., Li, W., Li, Y., An, Y., Wu, H., & Guo, Y. (2024). Effects of plant nutrient acquisition strategies on biomass allocation patterns in wetlands along successional sequences in the semi-arid upper Yellow River basin. *Frontiers in Plant Science,15*, Article 1441567. https://doi.org/10.3389/fpls.2024.1441567

Wigand, C., Roman, C. T., Davey, E., Stolt, M., Johnson, R., Hanson, A., Watson, E. B., Moran, S. B., Cahoon, D. R., Lynch, J. C., & Rafferty, P. (2014). Below the disappearing marshes of an urban estuary: Historic nitrogen trends and soil structure. *Ecological Applications, 24*(4), 633–649.

Wilson, C. A., Hughes, Z. J., & FitzGerald, D. M. (2022). Causal relationships among sea level rise, marsh crab activity, and salt marsh geomorphology. *Proceedings of the National Academy of Sciences, 119*(9), Article e2111535119. https://doi.org/10.1073/pnas.2111535119

Xu, X., Chen, M., Yang, G., Jiang, B., & Zhang, J. (2020). Wetland ecosystem services research: A critical review. *Global Ecology and Conservation, 22*, Article e01027. https://doi.org/10.1016/j.gecco.2020.e01027

Yang, W., An, S., Zhao, H., Xu, L., Qiao, Y., & Cheng, X. (2016). Impacts of *Spartina alterniflora* invasion on soil organic carbon and nitrogen pools sizes, stability, and turnover in a coastal salt marsh of eastern China. *Ecological Engineering, 86*, 174–182. https://doi.org/10.1016/j.ecoleng.2015.11.010

Zedler, J. B., & Kercher, S. (2005). Wetland resources: Status, trends, ecosystem services, and restorability. *Annual Review of Environment and Resources,30*(1), 39–74. https://doi.org/10.1146/annurev.energy.30.050504.144248

Zervas, C. (2001). *Sea level variations of the United States 1854–1999*. NOAA Technical Report NOS CO-OPS 36, 80 p. Retrieved January 8, 2025, from https://tidesandcurrents.noaa.gov/publications/NOAA_Technical_Report_NOS_COOPS_036.pdf